ARCHIWUM HYDROTECHNIKI
Tom Zeszyt

*LESZEK M. KACZMAREK, RAFAŁ OSTROWSKI**

Dynamics of wave–current bottom boundary layer
Part 1
Modelling turbulent boundary layer in nonlinear wave motion

Notation

c – wave celerity;
g – acceleration of gravity;
h – mean water depth;
H – wave height;
k_s – Nikuradse's roughness parameter;
L – wave length;
p – pressure;
t – time;
T – wave period;
u – instantaneous velocity;
u_c – current velocity;
u_d – defect velocity;
u_f – friction velocity;
$\hat{u}_f$ – equivalent maximum friction velocity;

*L. M. Kaczmarek (Ph.D.), R. Ostrowski (M.Sc.) – Institute of Hydroengineering of the Polish Academy of Sciences, Kościerska 7, 80–953 Gdańsk

u_{fc} – root mean square friction velocity;

U – free stream velocity;

w_∞ – induced vertical velocity at the top of boundary layer;

x – horizontal coordinate;

z – vertical coordinate:

z_0 – theoretical bed level;

$z_{\max}$ – validity limit of boundary layer equation of motion;

δ – boundary layer thickness;

δ_1 – boundary layer thickness at moment corresponding to maximum free stream velocity;

δ_2 – boundary layer thickness at moment corresponding to minimum free stream velocity;

κ – von Karman constant;

ν_t – eddy viscosity;

ρ – water density;

τ – shear stress;

τ_0 – bottom shear stress;

τ_c – shear stress averaged over time; region;

ω – angular frequency.

1. Introduction

Bottom shear stress due to motion ot water is commonly assumed to be the chief cause of the movement of sea bed grains. Because the concentration of sediment is biggest in the sea bed boundary layer, the sediment transport most intensive there. Therefore an accurate description of velocity and friction distributions in time and space, and especially a precise determination of their qualitative and quantitative characteristics is of crucial importance within the field of coastal engineering. The problem is extremely sophisticated because of nonlinear interactions between flow and sea bed.

One may distinguish at least three major types of interactions for for bottom shear stress:

- influence of bed roughness on velocity distribution in boundary layer
- interaction of suspended sediment and velocity in the boundary layer where suspension of sediment is shaped by bottom friction and in turn damps the turbulence inside the boundary layer affecting velocity distributions
- nonlinear interaction of waves and currents.

The above intercorrelations are partly reflected in the distribution of eddy viscosity ν_t (Kaczmarek & Ostrowski 1989, 1991):

$$\begin{aligned} \nu_t(z) &= \kappa \hat{u}_f z \quad \text{for} \quad && \tfrac{k_s}{30} \le z \le \tfrac{\delta_m}{4} + \tfrac{k_s}{30} \\ \nu_t(z) &= \kappa \hat{u}_f \left(\tfrac{\delta_m}{4} + \tfrac{k_s}{30}\right) \quad \text{for} \quad && z > \tfrac{\delta_m}{4} + \tfrac{k_s}{30} \end{aligned} \tag{1}$$

The formulae (1) are rooted in the hypothesis of Kajiura (1968) and the simplification of Brevik (1981) for rough turbulent boundary layer. Only turbulent regime of motion is considered here.

Within the above sheme the friction expressed by the friction velocity u_f is coupled with velocity distributions. The quantity $\hat{u}_f$ is an equivalent (characteristic) friction velocity dependent on $u_f(\omega t)$. The scheme implies that eddy viscosity distribution depends on roughness coefficient k_s, the parameter δ_m associated with the boundary layer thickness and correlated with friction velocity, and the von Karman constant κ assumed as 0.4 for clear water (decreasing in the pesence of suspended sediment.

Attention is focused only on the third of the specified interactions. One can distinguish four cases:

- linear wave over rough bed
- linear wave superimposed on current
- nonlinear wave over rough bed
- nonlinear wave superimposed on current.

The solution of the equation of motion in boundary layer for the first case has been proposed by Kaczmarek & Ostrowski (1989) and Kaczmarek (1990) who used the distribution (1). The second case has been recently discussed by Kaczmarek & Ostrowski (1991). Present paper deals with nonlinearities linked to wave motion only, while an approach concerning the interaction of nonlinear waves and currents will be presented in Part 2.

The relationships in boundary layer due to nonlinear wave are discussed in Section 2 of the current paper and the solution of equation of motion for asymmetric wave is provided in Section 3. Roughness k_s and parameter κ are assumed to be known and constant.

2. Identification of nonlinearities bound with wave motion

2.1. Mathematical description of wave and boundary layer

Wave theories are based on numerous simplifying assumptions such as potential motion, inviscid water, neglect of Coriolis force, etc.

Solutions provide potential functions of wave motion $\Phi(x,z,t)$. The potential function for Stokes 2nd order theory is given as:

$$\begin{aligned} \Phi(x,z,t) &= \frac{Hg}{2\omega}\frac{\cosh[k(h+z)]}{\cosh(kh)}\sin(kx-\omega t) - \\ &+ \frac{3}{32}\omega H^2 \frac{\cosh[2k(h+z)]}{\sinh^4(kh)}\sin[2(kx-\omega t)] \end{aligned} \tag{2}$$

The first term of the above formula is a solution to *linear* wave theory while the second term (nonlinear) expresses the dependence of potential function on a square of wave height (usually much smaller).

The approximations implied by the Stokes theory are particularly useful for the cases of short–period waves and small Ursell parameter $U = \frac{H}{h}(\frac{L}{h})^2 < 75$. However, for shallow water waves Stokes 2nd approximation there often appears an extra crest at wave trough. For such cases the use of higher order approximations, for instance the theory of Borgman and Chappelear, is recommended. In general one may find out that for the value of Ursell parameter greater than 40 it is necessary to take advantage of Stokes approximation of order higher than 2.

Incorporating Prandtl's postulates one obtains the following equations describing turbulent motion in boundary layer:

$$\begin{aligned} \frac{\partial u}{\partial x} + \frac{\partial w}{\partial z} &= 0 \\ \frac{\partial u}{\partial t} + \frac{\partial}{\partial x}(u^2) + \frac{\partial}{\partial z}(uw) &= -\frac{1}{\rho}\frac{\partial p}{\partial x} + \frac{\partial}{\partial z}(\nu_t \frac{\partial u}{\partial z}) \\ -\frac{1}{\rho}\frac{\partial p}{\partial x} &= \frac{\partial U}{\partial t} + \frac{\partial}{\partial x}(U^2) + \frac{\partial}{\partial z}(UW) \end{aligned} \tag{3}$$

in which U, W denote components of orbital velocity at the upper limit of boundary layer.

The system of Equations (3) is a system of nonlinear equations because of the presence of terms $\frac{\partial}{\partial x}(u^2)$, $\frac{\partial}{\partial z}(uw)$, $\frac{\partial}{\partial z}(UW)$, $\frac{\partial}{\partial x}(U^2)$, among which the term $\frac{\partial}{\partial x}(U^2)$ is associated with so called radiation stress (Longuet–Higgins & Stewart 1964), while the term $\frac{\partial}{\partial z}(UW)$ describes vertical momentum transfer caused by orbital motion.

In linear approximation, the term (UW), averaged over wave period, vanishes automatically in the entire the region of potential motion. Moreover, the correlation U^2 is neglected a priori. Hence the motion of water in boundary layer in linear approximation is governed by the following equation:

$$\frac{\partial u}{\partial t} = \frac{\partial U}{\partial t} + \frac{\partial}{\partial z}\left(\nu_t \frac{\partial u}{\partial z}\right) \tag{4}$$

Kaczmarek & Ostrowski (1989, 1991) proposed a solution of Eq. (4) with distributions of ν_t according to (1).

Within nonlinear approximation the term (UW), averaged over wave period, being different from zero in the region of potential motion, vanishes at the limit of boundary layer, similarly as for the linear approximation. Thus the equation of motion in the boundary layer has the form:

$$\frac{\partial u}{\partial t} + u\frac{\partial u}{\partial x} = \frac{\partial U}{\partial t} + U\frac{\partial U}{\partial x} + \frac{\partial}{\partial z}\left(\nu_t \frac{\partial u}{\partial z}\right) \tag{5}$$

Assuming that the velocity u does not depend on x, one may neglect the convective terms and simultaneously take the nonlinearity into account by expressing the velocities of bottom oscillations $U(t)$ in potential motion by nonlinear Stokes approximation. In this way the *asymmetry* of wave with respect to still water level is considered. Such an approach is presented in the next section.

2.2. Proposed description of friction in boundary layer due to nonlinear wave

Although a lot of solutions of boundary layer problem for and sinusoidal waves have been provided (Jonsson & Carlsen 1976, Brevik 1981, Fredsoe 1981, Kaczmarek & Ostrowski 1989) no vigorous mathematical description of the turbulent boundary layer is available for a wave form asymmetric with respect to still water level.

Equation (4) can be rewritten as:

$$\frac{\partial}{\partial t}(u-U)=\frac{1}{\rho}\frac{\partial \tau}{\partial z} \tag{6}$$

In order to define $u_f(t)$ the assumptions of Fredsoe's model (1981) formulated for sinusoidal wave and the suggestion of Fredsoe, Andersen & Silberg (1985) concerning the possibility of adaptation of the model for nonlinear wave case have been employed.

Eq. (6) after integration reads:

$$-\frac{\tau_0}{\rho}=-u_f^2=-\int\limits_{\frac{k_s}{30}}^{\delta+\frac{k_s}{30}}\frac{\partial}{\partial t}(U-u)dz \tag{7}$$

The assumption is made that the velocity profile in the boundary layer is described by the logarithmic function:

$$\frac{u}{u_f}=\frac{1}{\kappa}\ln\frac{30z}{k_s} \tag{8}$$

where the z axis is directed upwards from the bottom.

The boundary condition at the upper limit of the boundary layer reads $u=U$ at $z=\delta+\frac{k_s}{30}$. On the strength of Equation (8) one has:

$$\delta=\frac{k_s}{30}(e^{z_1}-1) \tag{9}$$

in which

$$z_1=\frac{U\kappa}{u_f} \tag{10}$$

After rearranging the integral on the right hand side of Eq. (7) one obtains:

$$-u_f^2=-\delta\frac{dU}{dt}+\frac{1}{\kappa}\frac{du_f}{dt}\frac{k_s}{30}[e^{z_1}(z_1-1)+1] \tag{11}$$

If one takes the derivative of Eq. (10):

$$\frac{dz_1}{dt}=\frac{z_1}{U}\frac{dU}{dt}-\frac{z_1}{u_f}\frac{du_f}{dt} \tag{12}$$

then one obtains the differential equation:

$$\frac{dz_1}{d(\omega t)}=\frac{30\kappa^2U(\omega t)}{k_s\omega e^{z_1}(z_1-1)+1}-\frac{z_1(e^{z_1}-z_1-1)}{e^{z_1}(z_1-1)+1}\frac{1}{U}\frac{dU}{d(\omega t)} \tag{13}$$

It is necessary to point out that the solution of Eq. (13) bases on an assumption that boundary layer develops anew every time the flow reverses. This implies the neglect of memory effects.

In our computations, the velocity at the upper limit of boundary layer is given by the second Stokes approximation:

$$U(\omega t) = \frac{HgT}{2L\cosh(\frac{2\pi h}{L})}\cos(\omega t) + \frac{3}{4}(\frac{\pi H}{L})^2\frac{L}{T}\frac{1}{\sinh^4(\frac{2\pi h}{L})}\cos(2\omega t) \tag{14}$$

Additionally the computations have encompassed the third Stokes approximation in the approach of Borgman and Chappelear:

$$U(\omega t) = F_1\cos(\omega t) + F_2\cos(2\omega t) + F_3\cos(3\omega t) \tag{15}$$

The coefficients F_1, F_2, F_3 are determined by iterative solution of the system of nonlinear equation given by Voogt (1979).

Equation (13) must be solved numerically. Because of the initial condition: $\delta = 0$ for $t = t_0$ (t_0 corresponds to the moment $U(\omega t_0) = 0$), the initial condition concerning the variable z_1 reads: $z_1 = 0$ for $t = t_0$. It leads to division by zero on the right hand side of Eq. (13). Therefore, for the first program step, a simplified form of Eq. (13) has been assumed – valid for times t not much varying from t_0:

$$\frac{dz_1}{d(\omega t)} = \frac{60\kappa^2 U(t_0 + \omega t)}{k_s\omega z_1^2} - \frac{z}{\omega t} \tag{16}$$

in which $U(z_0 + \omega t) = U_{mz}\omega t$.

The solution of Eq. (16) reads:

$$z_1 = \sqrt[3]{\frac{6}{5}\cdot\frac{30\kappa^2 U_{mz}}{k_s\omega}}(\omega t)^{\frac{2}{3}} \tag{17}$$

The solution of Eq. (13) has been obtained by the Runge–Kutta second–order method. As a result, the function $z_1(t)$ has been obtained and the time distributions of friction velocity $u_f(t)$ and boundary layer thickness $\delta(t)$ have been calculated thereafter on the basis of Equations (9) and (10).

The computations have been carried out for the parameters of a typical wave generated in laboratory: $h = 12.5$ cm, $H = 5$ cm, $T = 1$ s, $k_s = 2$ mm. Temporal distributions of the input $U(\omega t)$, the function $z_1(\omega t)$, friction velocity $u_f(\omega t)$ and boundary layer thickness $\delta(\omega t)$ for the cases of 2nd and 3rd Stokes approximations are depicted in Fig. 1. The influence of the asymmetry of bottom velocity oscillations on friction velocity u_f and turbulent boundary layer thickness δ is visible. The asymmetry of bottom velocity oscillations brings about non–uniform growth of boundary layer thickness in crest and trough phases, and accordingly non–uniform friction.

The presented computational procedure permits the determination of the characteristics of bottom friction (δ and u_f) practically for any input $U(t)$. The paper presents the application of the method for 2nd and 3rd Stokes approximation.

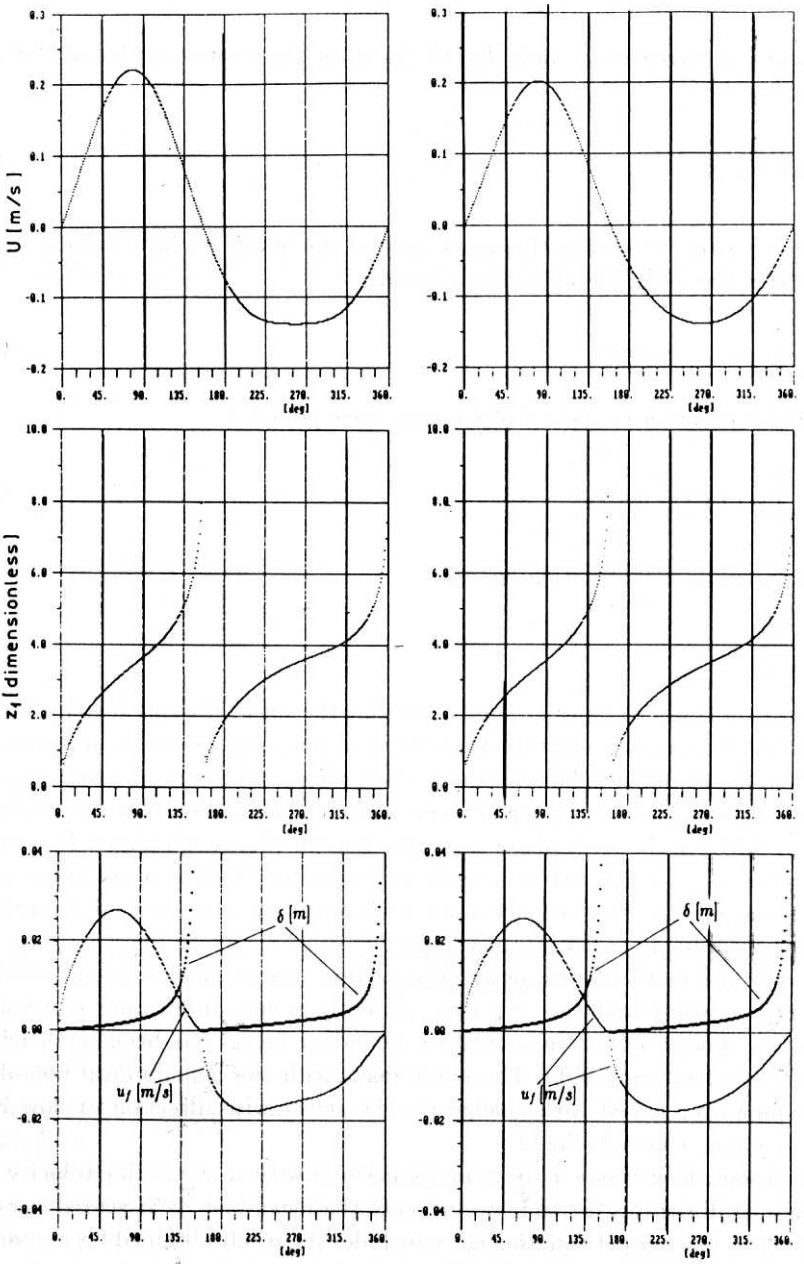

Fig. 1. $U(\omega t)$, $z_1(\omega t)$, $u_f(\omega t)$, $\delta(\omega t)$ for 2nd (left side) and 3rd (right side) Stokes approximation

The following relationship is valid for the analysed two cases, as for any other polyharmonic input:

$$\int_0^T U(t)dt = 0 \tag{18}$$

i.e. the resultant water velocity at the upper limit of the boundary layer is zero.

Making use of the definition of friction velocity:

$$u_f = \sqrt{\frac{\tau}{\rho}} \tag{19}$$

one may determine the mean shear stress within wave period T:

$$\tau_c = \frac{1}{T}\int_0^T \rho \mid u_f(t) \mid u_f(t)dt \tag{20}$$

and the corresponding mean friction velocity:

$$u_{fc} = \sqrt{\frac{\tau_c}{\rho}} \tag{21}$$

On the basis of computations one finds out that the mean friction velocity for an arbitrary nonlinear input is a positive value. In analysed cases, mean shear stress u_{fc}^2 has represented about 5% of maximum shear stress u_{fmax}^2, where $u_{fmax} = max[u_f(t)]$.

The above statement is very important as it leads to a conclusion that the resultant absolute shear stress in the crest phase is greater than in the trough phase. Hence the mean shear stress ρu_{fc}^2 is induced as a result of bottom oscillations asymmetry. This mean shear stress reflects the existence of a certain resultant current inside boundary layer, directed accordingly to wave propagation.

The research and mathematical description of this current has not been a subject of analysis in the world literature till now. Recently a very interesting *experimental* study on asymmetry effects in oscillatory boundary layers has been reported by Sumer, Fredsoe & Laursen (1991). The study deals with the non-uniform boundary layers developing over a bed with changes in the streamwise direction of flow in a converging-diverging channel (Fig. 2).

The free stream flow was a purely oscillating one with a sinusoidal velocity variation. Figure 3a illustrates the time evolution of the mean bed shear stress over one period of the flow. For comparison, the figure includes the result obtained for a uniform oscillatory boundary layer flow ($\beta = 0°$). The figure demonstrates that the shear stress increases in the convergent half-period and decreases in the divergent half-period compared to the values of the uniform oscillatory boundary layer flow. This indicates that the period-averaged bed shear stress $\overline{\tau_0}$ is non-zero in the case of convergent-divergent channel. As seen from the figure, this non-zero period-averaged shear stress is directed towards the converging direction. The latter implies that there is a constant streaming of fluid near the wall towards the converging end of the channel. Figure 3b gives the

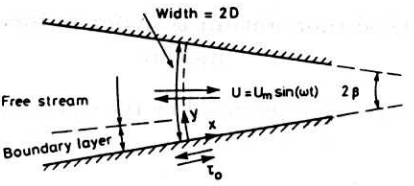

Fig. 2. Definition sketch. Oscillatory flow in convergent–divergent channel (Sumer et al. 1991)

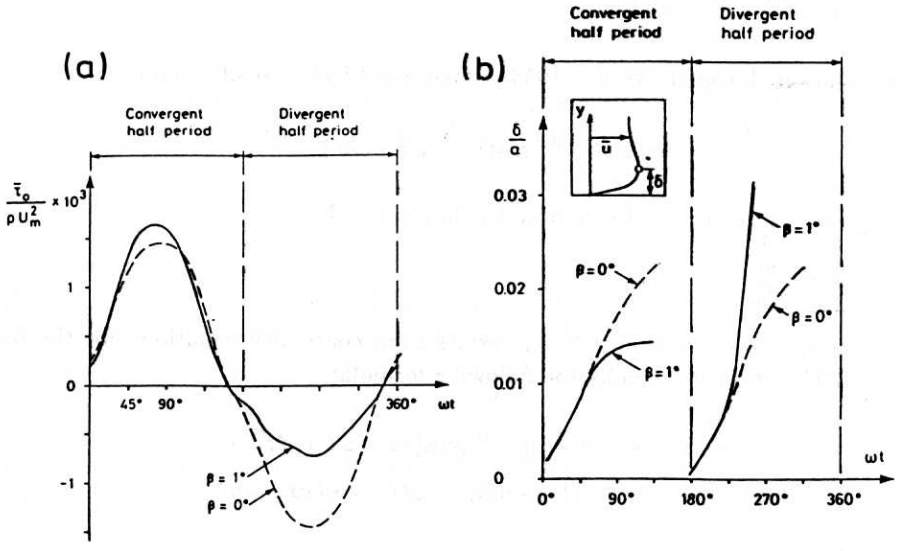

Fig. 3. Time evolution of mean shear stress (a) and boundary layer thickness (b) (Sumer et al. 1991)

boundary layer thickness plotted as a function of ωt. The boundary layer is rather thick in the divergent half–period, while the opposite is true for the convergent half–period of the flow.

All earlier attempts of *theoretical* description of the resultant current induced inside a boundary layer have led to the identification of wave–induced mass flux caused by the displacement in a boundary layer, see for example Hedegaard & Fredsoe (1984). This flux arises because a phase shift exists between the horizontal and vertical flow velocities at the top of the boundary layer in non–uniform water waves, so the term $\overline{UW}$ does not vanish. As shown by Longuet–Higgins (1953) the spatial and temporal gradients in the velocity deficit of the wave boundary layer creates a vertical velocity, which is small compared with the orbital velocities. This additional vertical velocity attains the value w_∞ outside the wave boundary layer, while it decreases through the boundary layer to be zero at the bed. This effect will be discussed in the next section.

2.3. Discussion of vertical momentum transfer induced by organized wave motion

For the laminar boundary layer described by the equation:

$$\frac{\partial \sigma}{\partial t} = \nu \frac{\partial^2 \sigma}{\partial z^2} \tag{22}$$

in which

$$\sigma = \frac{\partial u}{\partial z} - \frac{\partial w}{\partial x} \simeq \frac{\partial u}{\partial z} \tag{23}$$

the solution (Longuet–Higgins 1953) is expressed by the relationship:

$$u = -\omega \frac{H}{2} cosech(kh) \cdot e^{-\beta z'} \cos(kx - \omega t + \beta z') \tag{24}$$

where $z' = z + h$ is a distance from the bottom and

$$\beta = (\frac{\omega}{2\nu})^{\frac{1}{2}} \tag{25}$$

The non–zero vertical velocity results from continuity equation. For the laminar case this velocity is given by the following formula:

$$w = 2^{-\frac{1}{2}} \omega \frac{H}{2} R_w^{-\frac{1}{2}} cosech(kh)[e^{-\beta z'}(\cos(kx - \omega t + \beta z') + \\ + \sin(kx - \omega t + \beta z')] - \sin(kx - \omega t) - \cos(kx - \omega t) \tag{26}$$

where $R_w = \frac{\omega}{\nu k^2}$

The existence of this velocity indicates that an additional mean (within wave period) shear stress $\overline{uw}$ is generated inside the boundary layer. This stress attains the maximum value at the upper limit of the layer. It causes the disturbances in the region of potential flow, because – on the basis of considerations conducted in Section 2.1 – there is no vertical momentum exchange represented by the term $\overline{uw}$ in linear wave motion. The approach of Longuet–Higgins implies that the form of vertical velocity w induced by the vorticity depends on the linear solution (24). Moreover it can be easily shown that the shear stress induced outside the boundary layer is oriented in the direction of wave propagation and the velocity is smaller by order of magnitude than its linear counterpart.

In the case of turbulent motion, the determination of the additional shear stress generated inside the boundary layer requires, as in laminar motion, the knowledge of the linear solution of Eq. (4). This solution depends on the distribution of eddy viscosity ν_t.

Using the continuity equation and assuming:

$$\frac{\partial}{\partial x} = -\frac{1}{c}\frac{\partial}{\partial t} \tag{27}$$

one may determine the additional vertical velocity w_∞ outside the boundary layer from the formula:

$$w_\infty = -\frac{\partial}{\partial x}\int_{\frac{k_s}{30}}^{\frac{k_s}{30}+\delta}(u-U)dz = \frac{1}{c}\int_{\frac{k_s}{30}}^{\frac{k_s}{30}+\delta}\frac{\partial}{\partial t}(u-U)dz \tag{28}$$

After taking into account Eq. (6) integrated over the boundary layer thickness, Eq. (28) transforms into the form:

$$w_\infty = -\frac{\tau_0}{c\rho} = -\frac{u_f\,|\,u_f\,|}{c} \tag{29}$$

The wave boundary layer thus acts as a small periodic disturbance which travels along the bed with the phase velocity c of the wave motion. Such a travelling disturbance will generate a surface wave with increasing wave height in the direction of propagation. This developing wave causes a reduction of the total wave height in the x – direction, when it is combined with the basic wave.

Recently Deigaard & Fredsoe (1989) have explained the physical mechanism which extracts the energy from the outer potential flow and transports it to the wave boundary layer, where it is converted to turbulence and heat. Following them let us consider the progressive, linear shallow–water waves. The sea bed is horizontal and the only deformation of the waves is assumed to be caused by the energy dissipation in the wave boundary layer. The wave condition is steady and the only variation in wave height is in the direction of propagation.

The velocity w_∞ is associated with an additional water surface elevation of:

$$\zeta^* = \int w_\infty dt = -\int \frac{1}{c}u_f|u_f|dt \tag{30}$$

Longuet–Higgins (1953) used the displacement induced vertical velocity to explain the phenomenon of streaming. It is interesting to note that the perturbation ζ^* of the water surface is not in phase with the horizontal orbital velocity U.

ζ^* gives rise to an additional horizontal pressure gradient $\partial p^*/\partial x$, which for linear shallow–water waves is given by:

$$\frac{\partial p^*}{\partial x} = \rho g\frac{\partial \zeta^*}{\partial x} = -\frac{\rho g}{c}\frac{\partial \zeta^*}{\partial t} = \frac{\rho g}{c^2}u_f|u_f| \tag{31}$$

This pressure gradient carries out a resulting work on the horizontal orbital velocity of the wave motion. The time–averaged rate of work per unit bed area is given by:

$$W = -\frac{h}{T}\int_0^T \frac{\partial p^*}{\partial x}U dt = -h\frac{\rho g}{c^2}\overline{u_f|u_f|U} = -\rho\overline{u_f|u_f|U} \tag{32}$$

which is of exactly the same magnitude as the time–averaged rate of energy dissipation per unit area of the bed E in the wave boundary layer defined as:

$$E = \frac{1}{T}\int_0^T U\tau dt = \rho\overline{Uu_f|u_f|} \tag{33}$$

The energy dissipated in the wave boundary layer is thus extracted from the outer wave motion through the work done against the pressure gradient associated with the additional surface elevation, caused by the displacement in the wave boundary layer.

The extraction of energy given by Eq. (32) is evenly distributed over the depth. As the dissipation takes place in the bottom boundary layer, energy must be transferred from the outer flow to the boundary layer. The downward energy transport is secured by the work done by the hydrostatic pressure on the vertical flow velocity. This time–averaged rate is calculated as:

$$W = -\rho g \overline{(\zeta + \zeta^*)\left(\frac{z}{h}\frac{\partial \zeta}{\partial t} + w_\infty\right)} = -\rho g \overline{\left(\zeta w_\infty + \zeta^* \frac{z}{h}\frac{\partial \zeta}{\partial t}\right)} \tag{34}$$

$\overline{\zeta \frac{\partial \zeta}{\partial t}}$ and $\overline{w_\infty \zeta^*}$ $(= \overline{\zeta^* \frac{\partial \zeta^*}{\partial t}})$ are zero as the waves are periodic. Hereby Eq. (34) becomes:

$$\begin{aligned} W &= \rho g \zeta \overline{\frac{u_f|u_f|}{c}} + \rho g \frac{z}{h} \overline{\frac{\partial \zeta}{\partial t} \int \frac{u_f|u_f|}{c} dt} \\ &= \rho g \zeta \overline{\frac{u_f|u_f|}{c}} + \rho g \frac{z}{h} \overline{\left[\frac{\partial}{\partial t}\left(\zeta \int \frac{u_f|u_f|}{c} dt\right) - \zeta \frac{u_f|u_f|}{c}\right]} \\ &= \rho g h \overline{\frac{\zeta c}{h}\frac{u_f|u_f|}{c^2}}\left(1 - \frac{z}{h}\right) = \rho \overline{U u_f|u_f|}\left(1 - \frac{z}{h}\right) \end{aligned} \tag{35}$$

which at the bed is equal to the work found in Eq. (32), i.e. all the energy extracted from the wave motion is transferred to the wave boundary layer.

The above considerations reveal that the nonlinearities bound with the generation of an additional vertical velocity w_∞ at the top of boundary layer i.e. the nonlinearities linked with the terms $\overline{UW}$ are closely associated with the dissipation of wave energy. Thus if the energy dissipation is neglected one may skip the additional stresses generated at the top of the boundary layer (a current induced by these stresses does not exist).

Considering the dissipative waves one should provide a solution for perturbated wave conditions. Although Deigaard & Fredsoe (1989) have obtained a solution using the perturbation analysis, the problem is still unsolved for the situation of zero mean discharge. For such a situation the problem reduces to the determination of the mean current distribution in the outer region of flow.

Finally it is worthwhile pointing out that the stress $\overline{uw_\infty}$ equals zero at the bottom and reaches the maximum value at the top of boundary layer while the effects of wave asymmetry play the key role very close to the bottom.

The above conclusions will be very helpful for formulation of a model in Section 3.

3. Velocity and shear stress in nonlinear wave boundary layer

3.1. Theoretical basis of present model

The first theoretical attempt of description of bottom boundary layer under nonlinear wave motion was presented by Tanaka 1989. He modified and extended the stream

function theory proposed by Dean for rotational and nonlinear waves. Dean's stream function theory was modified to include the effect of the turbulent viscosity. Although that approach provides the instantaneous velocity profiles for the case of nonlinear wave, the induced mean flow in the boundary layer has not been considered. Contrary to the recalled approach, the Authors propose a theoretical solution which deals with the nonlinear effects represented by the additional current generated inside the boundary layer.

Within the current approach, the nonlinearity of the phenomenon is represented by the asymmetry of wave input (oscillatory horizontal velocity $U(t)$ at the upper limit of boundary layer) described by 2nd and 3rd Stokes approximation. The temporal distributions of friction velocity $u_f(\omega t)$ and boundary layer thickness $\delta(\omega t)$ are computed with the procedure presented in Section 2.2. Then the equation of motion (4) is solved numerically and the velocity $u(z,t)$ inside boundary layer is determined for $z = z_0 \rightarrow z_{max}$ and $t = t_0 \rightarrow (t_0 + T)$, where $z_0 = k_s/30$ and t_0 corresponds to the instant of $U(t) = 0$. The upper limit z_{max} has been estimated as $z_{max} \approx 2\delta_m + k_s/30$ (Kaczmarek, Ostrowski 1989), and $\delta_m = max(\delta_1, \delta_2)$ is the mean boundary layer thickness, where δ_1 and δ_2 are the boundary layer thicknesses at the times corresponding to maximum and minimum oscillatory input, respectively. In the end, the mean current distribution u_c is calculated and superimposed on the instantaneous velocity profiles.

Eq. (4) is solved numerically by an implicit method involving the Crank – Nicholson scheme. Introducing the defect velocity $u_d(z,t) = u(z,t) - U(t)$ one has:

$$\frac{\partial u_d}{\partial t} = \frac{\partial}{\partial z}\left(\nu_t \frac{\partial u_d}{\partial z}\right) \tag{36}$$

The following approximate initial condition is assumed:

$$u_d(z, t_0) = 0 \tag{37}$$

and the boundary conditions are:

$$u_d(z_0, \omega t) = -U(\omega t) \tag{38}$$

$$u_d(z_{max}, \omega t) = 0 \tag{39}$$

Because the approximate initial condition (37) has been involved, the computations have had to cover the time corresponding to a few wave periods until the compatibility between $u_d(z, t_0 + N \cdot T)$ and $u_d[z, t_0 + (N+1) \cdot T]$. The number of required runs N depends on wave parameters and is three to five.

As a result of computations by the procedure presented in Section 2.2, an additional mean shear stress τ_c and corresponding friction velocity u_{fc} appear. Using the extrema in friction velocity distribution (Fig. 1) the equivalent maximum friction velocity $\hat{u}_f$ (employed in the eddy viscosity distribution (1)) is defined as:

$$\hat{u}_f = [0.5(u_{fmax}^2 + u_{fmin}^2]^{\frac{1}{2}} \tag{40a}$$

Alternatively, one may assume:

$$\hat{u}_f = max(u_{fmax}, |u_{fmin}|) \tag{40b}$$

cf. Kaczmarek, Ostrowski (1991).

The assumption has been made that in a certain limited region in the close vicinity of the bed the shear stress τ_c is constant. This assumption is very realistic but the thickness of the region is questionable. The choice is rather arbitrary. The Authors propose the upper limit of this region as the ordinate corresponding to the level at which the mean of maximum and minimum velocity profiles reaches the free stream velocity. In accordance with Jonsson & Carlsen (1976), $\delta_m/2 + k_s/30$ is the most consistent measure (see discussion Kaczmarek, Ostrowski 1991).

Basing on Boussinesq's hypothesis, eddy viscosity distribution (1) and the definition of friction velocity (21) one may formulate the following equation:

$$\kappa \hat{u}_f z \frac{du_c}{dz} = u_{fc}^2 \tag{41}$$

in the range $< k_s/30; \delta_m/4 + k_s/30 >$ and

$$\kappa \hat{u}_f \left(\frac{\delta_m}{4} + \frac{k_s}{30} \right) \frac{du_c}{dz} = u_{fc}^2 \tag{42}$$

in the range $(\delta_m/4 + k_s/30; \delta_m/2 + k_s/30 >$.

In Eqs. (41) and (42) the quantity u_c is a mean current resulting from the existence of the additional friction ρu_{fc}^2. Integrating Equations (41), (42) and taking advantage of the condition $u_c(z = k_s/30) = 0$ one comes up with the formulae:

$$u_c(z) = \frac{u_{fc}^2}{\kappa \hat{u}_f} ln \frac{z}{ks/30} \tag{43}$$

in the range $< k_s/30; \delta_m/4 + k_s/30 >$ and

$$u_c(z) = \frac{u_{fc}^2}{\kappa \hat{u}_f} \left(\frac{z}{\delta_m/4 + k_s/30} + ln \frac{\delta_m/4 + k_s/30}{k_s/30} - 1 \right) \tag{44}$$

in the range $(\delta_m/4 + k_s/30; \delta_m/2 + k_s/30 >$.

In the range $(\delta_m/2 + k_s/30; z_{max})$, the mean current distribution decreases linearly upwards on the assumption that the boundary conditions at the top of boundary layer with respect to continuity of velocity must be satisfied. The velocity at $z = \delta_m/4 + k_s/30$ is determined by the formula (44) while the velocity at $z = z_{max}$ must be given explicitly. In the presented simplified model the latter is assumed as zero, but one should be aware of the fact that thus the vertical momentum transfer represented by the term $\overline{uw}$ is neglected (cf. Section 2.3). The effect of $\overline{uw}$ term will be discussed with respect to the case of wave and current interaction in Part 2 of the paper.

Hence the mean current velocity in the layer $(\delta_m/2 + k_s/30; z_{max})$ reads:

$$u_c(z) = \frac{u_{fc}^2}{\kappa \hat{u}_f} \left(ln \frac{\delta_m/4 + k_s/30}{k_s/30} + 1 - \frac{z - \delta_m/2 - k_s/30}{1.5\delta_m} \right) \tag{45}$$

After superimposing the mean current velocity distribution on all the instantaneous velocity profiles the bottom shear stress may be determined. Integrating the equation of motion:

$$\frac{\partial u_d}{\partial t} = \frac{1}{\rho}\frac{\partial \tau}{\partial z} \tag{46}$$

over a certain height Δz

$$\int_{\frac{k_s}{30}}^{\frac{k_s}{30}+\Delta z} \frac{\partial u_d}{\partial t} dz = \frac{1}{\rho} \int_{\frac{k_s}{30}}^{\frac{k_s}{30}+\Delta z} \frac{\partial \tau}{\partial z} dz \tag{47}$$

the bottom shear stress formula is obtained:

$$\tau_{\frac{k_s}{30}} = \tau_{\frac{k_s}{30}+\Delta z} - \rho \int_{\frac{k_s}{30}}^{\frac{k_s}{30}+\Delta z} \frac{\partial u_d}{\partial t} dz \tag{48}$$

in which the first right hand term is calculated accordingly to Eq. (1) and Boussinesq's hypothesis:

$$\tau_{\frac{k_s}{30}+\Delta z} = \rho \kappa \hat{u}_f \left(\frac{k_s}{30} + \Delta z\right) \left.\frac{\partial (u_d + u_c)}{\partial z}\right|_{z=\frac{k_s}{30}+\Delta z} \tag{49}$$

whereas the second right hand term of (48) is expressed by Simpson's formula for numerical integration of the function $y(x)$ with a step Δx in a range $< a; b >$ (for an even number n of intervals):

$$\int_a^b y dx \approx \frac{1}{3}\Delta x (y_0 + 4y_1 + 2y_2 + 4y_3 + \ldots + 2y_{n-2} + 4y_{n-1} + y_n) \tag{50}$$

The quantity Δz should equal the total thickness of validity of Eq. (46) i.e. $2\delta_m$. In fact it has been limited to small value corresponding to the region in which the computed velocity profiles fit the measured ones best.

3.2. Comparison between theory and measurements

The laboratory experiment of van Doorn and Godefroy (1978) has been considered. The measurements were carried out in an open glass–walled wave flume with horizontal bottom, 30 m long, 0.5 m wide, with the net length for the waves in the flume (between wave board and wave damper) of about 26 m. The tests including velocity measurements were carried out under the following conditions: still water depth $h = 0.3$ m, wave period $T = 2$ s, wave height $H = 0.12$ m. Conditions for a turbulent wave boundary layer were created by artificial roughness elements fixed to the bottom in the measuring section.

For the comparison, the wave input has been assumed at first as 3rd Stokes approximation given by the theory of Borgman and Chappelear, Fig. 4.

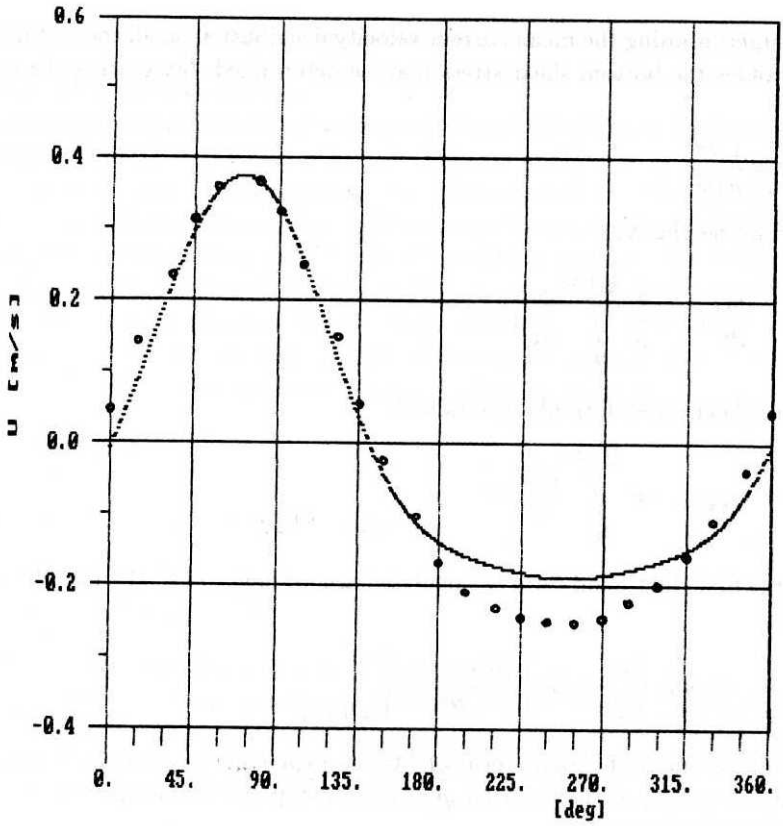

Fig. 4. Measured (o) and calculated (–) wave input $U(\omega t)$

The measurements have not revealed any mean current velocity near the top of boundary layer i.e. no dissipative effects have existed. This is confirmed by the registrations of free surface elevation $\zeta(t)$ which have shown an average negative value of $2 \div 3$ mm. The missing water has been stored in front of the wave train resulting in set–down and a small return current in the outer region of the flow, the presence of which has been found out by van Doorn & Godefroy (1978). The mathematical description of such a type of currents has been proposed by Kaczmarek & Szmytkiewicz (1991).

Before comparison, two values should be determined, the theoretical bed level and Nikuradse's equivalent roughness parameter k_s $(= 30z_0)$. In case of the flow over a rough bottom, it has been empirically found that the theoretical bed level is located somewhat lower than the top of the roughness element, e.g. Jonsson & Carlsen (1976). However, no method is available to estimate the displacement of the theoretical bed level and the height of the equivalent roughness under an oscillatory motion. The roughness parameter has been recommended to be determined experimentally by fitting

the measured velocity profile near the bottom to a logarithmic profile. In this study the quantity k_s has been estimated as 3.5 cm.

With the use of the procedure presented in Section 2.2 the boundary layer thickness $\delta(\omega t)$ and the bottom friction velocity $u_f(\omega t)$ have been computed (method *a*). The friction velocity has also been determined by the use of Eqs. (48), (49), (50) and (19) (method *b*). The results are depicted in Fig. 5.

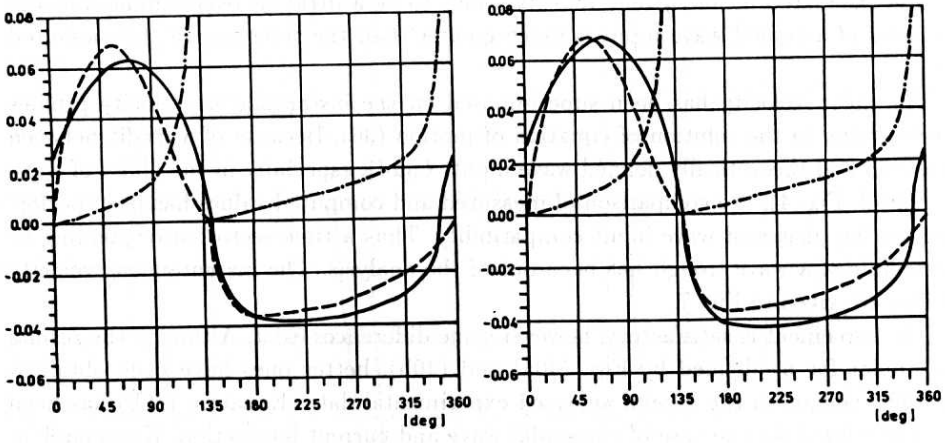

Fig. 5. Temporal distributions of $\delta(\omega t)$ (- · -), $u_f(\omega t)$: method *a* (- -), method *b* (–) for $\hat{u}_f$ by Eq. (40a) (left) and Eq. (40b) (right)

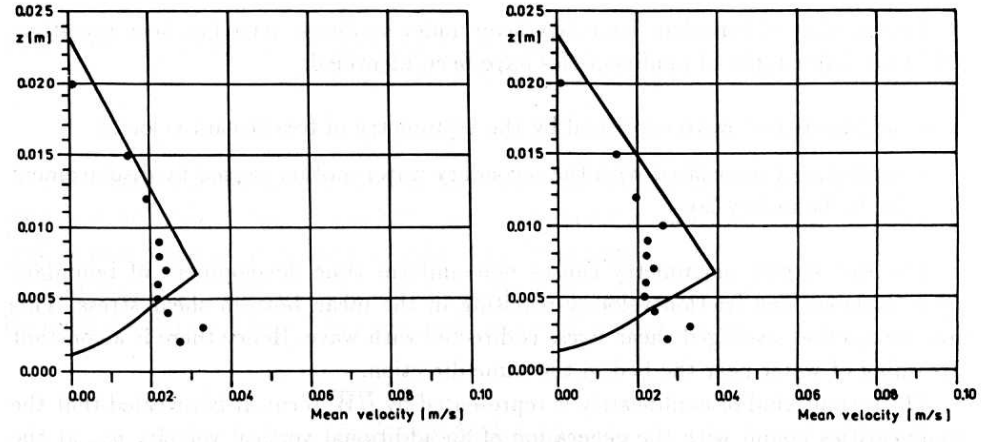

Fig. 6. Measured (•) and postdicted (–) mean velocity distribution for $\hat{u}_f$ by Eq. (40a) (left) and Eq. (40b) (right)

Both methods (a) and (b) provide nearly the same maximum and minimum values of $u_f(\omega t)$. The most important advantage of method (b) is that it provides a phase shift between $u_f(\omega t)$ and $U(\omega t)$ of order not exceeding 30° (in the phase of wave trough) and about 0° (in the phase corresponding to transition from crest to trough when a small instantaneous velocity at the bottom acts against the mean current).

The mean current velocity profile has been calculated on the basis of the formulae (43), (44), (45) and is plotted together with measured values in Fig. 6.

The calculated mean current velocity seems to be a little bit overestimated as the steepness of assumed wave input is much greater than the steepness of the measured one.

The mean velocity has been superimposed on the instantaneous velocity profiles obtained due to the solution of equation of motion (36). Because of a misfit between measured and theoretically defined wave inputs $U(\omega t)$, especially in the phase of wave trough (cf. Fig. 4), the comparison of measured and computed values has been performed for the phases of wave input compatibility. Thus a time sector corresponding to the middle of a wave trough has been out of the analysis. The instantaneous velocity profiles are given in Fig. 7.

The agreement is satisfactory, however some differences exist. Although the results are similar for $\hat{u}_f$ defined by Eqs. (40a) and (40b), better ones have been obtained for (40b) version in the case of analysed experimental data. Equation (40b) has been previously used for the case of sinusoidal wave and current interaction, Kaczmarek & Ostrowski (1991), and the comparison with available laboratory data has been quite good.

4. Conclusions

The problem of turbulent boundary layer under nonlinear wave has been investigated. Two major types of nonlinearities have been identified:

- nonlinearity of wave expressed by the asymmetry of free stream velocity
- nonlinearity associated with the secondary water motion caused by displacement in the boundary layer.

The free stream asymmetry causes non–uniform time development of boundary layer thickness and friction velocity resulting in the mean bottom shear stress. This non–zero period–averaged shear stress is directed with wave. Hence there is a constant streaming of water near the bed in the same direction.

The second kind of nonlinearity is represented by $\overline{UW}$ term. It is revealed that the nonlinearities bound with the generation of an additional vertical velocity w_∞ at the top of boundary layer are closely associated with the dissipation of wave energy. As far as the energy dissipation in the boundary layer is neglected one may skip the additional stresses generated at the top of boundary layer (linked with the terms $\overline{Uw_\infty}$. In any other case, for dissipative waves, the additional current is induced.

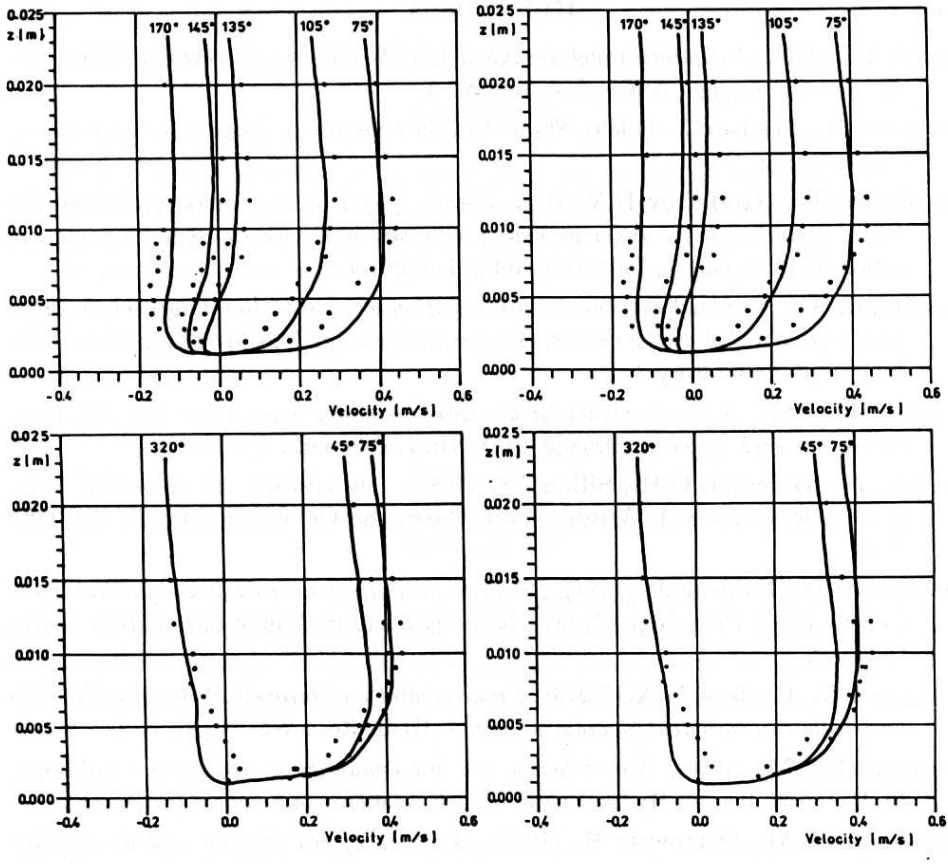

Fig. 7. Measured (•) and postdicted (–) instantaneous velocity distributions for $\hat{u}_f$ by Eq. (40a) (left) and Eq. (40b) (right)

The mathematical model of boundary layer for nonlinear wave input has been proposed. It enables one to calculate the instantaneous and mean current velocity profiles and temporal distributions of bottom shear stress.

The results of computations are compared with laboratory measurements of van Doorn & Godefroy (1978). The agreement seems to be satisfactory.

Acknowledgements

The study has been sponsored by KBN and PAN, Poland, under programme 2 IBW PAN, which is hereby gratefully acknowledged. The Authors wish to thank Prof. R. Zeidler for the discussions and helpful suggestions throughout the study.

References

Brevik I. (1981), *Oscillatory rough turbulent boundary layers*, J. Wtrway., Port, Coast. and Oc. Engng., ASCE, Vol. 107, No 3.

Deigaard R., Fredsoe J. (1989), *Shear stress distribution in dissipative water waves*, Coast. Engng., No 13.

van Doorn Th., Godefroy H.W.H.E. (1978), *Experimental investigation of the bottom boundary layer under periodic progressive water waves*, Report on investigation M 1362, part 1, Delft Hydraulics Laboratory.

van Doorn Th. (1981), *Experimental investigation of near–bottom velocities in water waves without and with a current*, Report on investigations M 1423, part 1, Delft Hydraulics Laboratory.

Fredsoe J. (1981), *A simple model for the wave boundary layer*, Prog. Rep. 54, Inst. Hydrodyn. and Hydraulic Engng. Tech. Univ. Denmark.

Fredsoe J., Andersen O.H., Silberg S. (1985), *Distribution of suspended sediment in large waves*, J. Wtrway., Port, Coast. and Oc. Engng., ASCE, Vol. 111, No 6.

Hedegaard B., Fredsoe J. (1984), *Resulting sediment transport due to nonlinear effects in waves*, Prog. Rep. 61, Inst. Hydrodyn. and Hydraulic Engng. Tech. Univ. Denmark.

Jonsson I.G., Carlsen N.A. (1976), *Experimental and theoretical investigations in an oscillatory turbulent boundary layer*, J. Hydr. Res., Vol. 14, No 1.

Kaczmarek L.M. (1990), *Non–cohesive sea bed dynamics in real wave conditions*, Ph.D. thesis, Inst. of Hydro–Engng. Polish Academy of Sciences (in Polish).

Kaczmarek L.M., Ostrowski R. (1989), *Analysis of bed friction and description of shear stress transmission into sea bed*, Report, Inst. of Hydro–Engng. Polish Academy of Sciences (in Polish).

Kaczmarek L.M., Ostrowski R. (1991), *Modelling of wave–current boundary layers with application to surf zone*, Hydrotechnical Archives, Vol. XXXIX, No 1–2.

Kaczmarek L.M., Szmytkiewicz M. (1991), *Mechanisms of generation of return flows in coastal zone*, Hydrotechnical Archives, Vol. XXXIX, No 1–2 (in Polish).

Longuet–Higgins M.S. (1953), *Mass transport in water waves*, Philos. Trans. R. Soc. London, Ser. A, 245: 535–581.

Longuet–Higgins M.S., Stewart R.W. (1964), *Radiation stress in water waves: A physical discussion with applications*, Deep Sea Res. Oceanogr. Abstr. 11, 529–562.

Sumer B.M., Fredsoe J., Laursen T.S. (1991), *Experimental studies on non–uniform oscillatory boundary layers*, Procs. of Euromech 262 Colloquium on Sand Transport in Rivers, Estuaries and the Sea, Wallingford, 26 – 29 June 1990.

Tanaka H. (1989), *Bottom boundary layer under nonlinear wave motion*, J. Wtrway, Port, Coast. and Oc. Engng., ASCE, Vol. 115, No 1.

Voogt W.J.P. (1979), *A numerical comparison of some water-wave theories*, Report on investigation R 1314, Delft Hydraulics Laboratory.

Summary

The mathematical model of boundary layer for nonlinear wave input has been proposed. It enables one to calculate the instantaneous and mean current velocity profiles and temporal distribution of bottom shear stress.

The results of computations are compared with laboratory measurements of van Doorn & Godefroy (1978). The agreement seems to be satisfactory.

Streszczenie

Dynamika falowo – prądowej warstwy przyściennej
Część 1
Modelowanie turbulentnej warstwy przyściennej w warunkach falowania nieliniowego

W pracy przebadano zachowanie się turbulentnej warstwy przyściennej w warunkach falowania nieliniowego. Przedstawiono model obliczający chwilowe i średnie rozkłady prędkości oraz chwilowe rozkłady naprężeń stycznych w warstwie przyściennej z uwzględnieniem efektów nieliniowości falowania. Wyniki obliczeń porównano z danymi laboratoryjnymi van Doorna i Godefroy (1978) otrzymując dobrą zgodność.